Original Article/นิพนธ์ต้นฉบับ

The Imaging Findings of the Brain Lesions in Adult HIV Patients at Ramathibodi Hospital

Wiboon Suriyajakryuththana[1], Wannita Mayurasakorn[1], Angsana Phuphuakrat[2], Pawin Numthavaj[3]

[1] *Department of Diagnostic and Therapeutic Radiology, Faculty of Medicine Ramathibodi Hospital, Mahidol University, Bangkok, Thailand*

[2] *Department of Medicine, Faculty of Medicine Ramathibodi Hospital, Mahidol University, Bangkok, Thailand*

[3] *Section for Clinical Epidemiology and Biostatistics, Faculty of Medicine Ramathibodi Hospital, Mahidol University, Bangkok, Thailand*

Abstract

Background: The central nervous system (CNS) is major targets of HIV. Imaging plays major role for diagnosis. In the era of highly active antiretroviral therapy (HAART), immune reconstitution inflammatory syndrome (IRIS) frequently develops, causing worsening of opportunistic infection after initial of HAART and atypical imaging findings.

Objective: To evaluate radiographic findings of HIV-related brain lesions and imaging characteristics in CNS-IRIS at Ramathibodi Hospital.

Methods: Adult HIV patients who performed the first CT of the brain and first MRI of the brain were reviewed. The final diagnoses from medical records were assessed followed by CSF analysis, pathological report, and therapeutic treatment.

Results: Eighty-one HIV patients (64 CT brains and 44 MRI brains) with HIV-related brain lesions were diagnosed. There were 24.7% cryptococcal infection, 18.5% tuberculous infection, 8.6% HIV encephalopathy and progressive multifocal leukoencephalopathy (PML), 7.4% neurosyphilis, 6.2% toxoplasmosis and TB-IRIS, 2.5% primary CNS lymphoma, and others.

Conclusions: Cryptococcal infection was the most common disease of adult HIV-related brain lesions followed by tuberculous infection, HIV encephalopathy, and PML. Besides less basal meningitis and hydrocephalus in tuberculous meningitis and no demonstrated target lesion in tuberculoma compared with prior literatures, other imaging findings of each HIV-related brain lesions were not different from those of the prior studies.

Keywords: CT, MRI, HIV, Immune reconstitution inflammatory syndrome, Highly active antiretroviral therapy

Corresponding Author: Wiboon Suriyajakryuththana

Department of Diagnostic and Therapeutic Radiology, Faculty of Medicine Ramathibodi Hospital, Mahidol University, 270 Rama VI Road, Ratchathewi, Bangkok 10400, Thailand.

Telephone: +66 2201 1259 E-mail: wiboonsuriya@yahoo.com

Introduction

The human immunodeficiency virus (HIV), retrovirus that infects cells of the immune system and disrupts their functions, known as one of the world major health problems.[1] According to the Joint United Nations program on HIV/AIDS (UNAIDS), an estimated of 36.9 million people were living with HIV infection at the end of 2014.[2]

Due to the ability to cross the blood-brain barrier in the early course of infection, central nervous system (CNS) is one of the major target of HIV.[1] The prevalence of neurological complication in HIV patients were estimated to be 39 - 70%,[3] and it was the first manifestation of symptomatic HIV infection in 10 - 20% of patients. In a review of autopsies of acquired immune deficiency syndrome (AIDS) patients, they also found 63% patients with abnormal pathology of the brain.[4]

Clinical presentations in HIV-related brain diseases show low diagnostic ability due to non-specific symptom for each disease. Investigations, such as the T-helper/inducer count (CD4 count) and standard test of cerebrospinal fluid (CSF cell count, cell differentiation, protein, and sugar) are also non-specific. Although CSF serology specific agent, CSF culture, and polymerase chain reaction (PCR) have high specificity, their sensitivities are only about 56 - 60%.[5] Brain biopsy, a reference standard for diagnosis, is an invasive procedure and not widely available. So then the use of it is still limited.

The diagnostic imaging still plays major role in diagnosis of HIV-related brain lesions. The imaging modalities, including computed tomography (CT), magnetic resonance imaging (MRI), single-photon emission computed tomography (SPECT), and positron emission tomography (PET) were performed to assist confirmation of diagnosis and selection of suitable treatment protocol.[6] Among them MRI is the modality of choice, dues to high sensitivity in lesion detection and differentiation. However, because CT scan is non-complicated, fast, relatively low cost, and widely available it is used as the first-line imaging modality for detection brain lesion, screening other life-threatening conditions, and screening contraindication prior to lumbar puncture in HIV patients.

Owing to highly active antiretroviral therapy (HAART) era, patients who suffered from HIV infection have better prognosis and life expectancy. However immune reconstitution inflammatory syndrome (IRIS), known as immune restoration disease, develops as a complication of HAART causing transient worsening of opportunistic infection after initiation of therapy and atypical imaging findings in HIV-related brain lesions such as contrast enhancement, interstitial edema, mass effect, and restricted diffusion in infections not typically characterized by these findings.[7-8]

This study aimed to evaluate radiographic findings of the HIV-related brain lesions and the imaging characteristics in CNS-IRIS.

Brain Lesions in HIV Patient

The spectrum of brain lesions in HIV patients can be broadly categorized into five groups: primary effect from HIV infection itself, secondary opportunistic infection, neoplasms, vascular diseases, and drug-related complication of treatment.

In countries where HAART is available, cognitive dysfunction caused directly by HIV itself, AIDs dementia complex or HIV encephalopathy (HIVE), represent the majority of cases.[9-10] In other areas, the opportunistic infections, which included progressive multifocal leukoencephalopathy (PML), cytomegalovirus (CMV) infection, cerebral toxoplasmosis, tuberculosis, cryptococcal infection, neurosyphilis, herpes simplex virus (HSV), bacterial meningitis, and other fungal infection, play the major role.

The primary CNS lymphoma (PCNSL) is HIV-associated neoplasm, which is the second most common brain mass found about 6% in HIV patients.[6] CNS disorder caused by HIV-associated vasculopathy is diagnosis of exclusion. Almost every pattern and type of vasculitis of small, medium and large vessels has been encountered in the HIV setting. IRIS known as immune restoration disease, is a complication of HAART that causes transient worsening

of opportunistic infection after initiation of therapy.

Methods

Retrospective, cross-sectional study was approved by institutional research ethics committee. The authors reviewed all CT and/or MRI brain before treatment of the brain lesions in HIV patients (seropositive), age ≥ 18 years, at Ramathibodi Hospital from January 2010 to August 2016 and had final diagnosis which was HIV-related brain lesion. The patients who had missing or inadequate data or non HIV-related brain lesions were excluded.

Imaging Techniques

***CT Imaging Techniques*:** The plain and contrasted axial CT scan of the brain were obtained with Aquilion one 320, (Toshiba, Japan), Somatom Sensation Cardiac 64, (Siemens, Germany), Aquilion CX 64, (Toshiba, Japan), and Extended Brilliance 256, (Philips, Netherlands), using the whole brain scan 3-mm slice thickness. 50-cc of intravenous non-ionic contrast material was administered and contrasted axial study was performed immediately after complete injection of contrast media.

***MRI Imaging Techniques*:** The standard protocols of MRI of the brain, included sagittal T1W MDEFT, sagittal and axial flair FS with Gd, axial SE T1W with and without Gd, axial TSE T2WFS, axial DWI B0 and B1000 with ADC mapping, axial SWI, coronal T2W FFE, THRIVE T1W FS with Gd in 3 planes, were obtained with Philips MR system Ingenia 3.0T, (Best, Netherland), GE Medical system Excite HDxt 1.5T, (Milwankee, USA), and Philips MR system Achieva 1.5T, (Best, Netherland). Intravenous gadolinium was administered using average dose of 0.1 mmol/kg.

Imaging Interpretations

The images were interpreted seperately by a third-year radiology resident in training and a board-certified neuroradiologist. If the interpretation were different, the images were re-evaluated by both interpretators and the results were reached by consensus. The final imaging interpretaion were recorded using data collection form described as follows.

***CT Imaging Findings*:**

1) Distribution: classify as no lesion, focal or diffuse lesions;

2) Number of lesion: classify as no lesion, single or multiple lesions.

3) Atrophy: define as presence of brain parenchymal volume loss with compensatory enlargement of the cerebrospinal fluid (CSF) space.

4) Non-enhanced findings: different density of the lesion compared with the normal tissue of the brain itself is classified as no lesion, hypodense, isodense, or hyperdense lesion.

5) Contrast-enhancement: on the basis that each brain lesion may show different characteristic enhancement. The contrast enhancement pattern after contrast administration is classified as no enhancement, homogeneous, heterogeneous, rim enhancement, and target sign patterns. The target sign is defined as a ring-shaped zone of peripheral enhancement with a small eccentric enhancing nodule.

6) Mass effect: define as phenomenon in which brain lesion causes surrounding areas of brain structures to be compressed due to space taking lesion.

7) Leptomeningeal enhancement: define as enhancement of the pia mater or enhancement that extends into the subarachnoid spaces of the sulci and cisterns.

8) Ventriculitis: define as inflammation of ventricles in the brain, seen as ventricular debris, periventricular or ependymal enhancement.

9) Hydrocephalus: define as an abnormal expansion of cavities (ventricles) within the brain that is caused by the accumulation of CSF.

***MRI Imaging Findings*:**

1) Distribution: classify as no lesion, focal or diffuse lesions.

2) Number of lesion: classify as no lesion, single or multiple lesions.

3) Atrophic: define as presence of brain parenchymal volume loss with compensatory enlargement of the CSF space.

4) T1W findings: on the T1W imaging, different signal of the lesion compared with the normal tissue of the brain itself is classified as no lesion, hypointense, isointense or hyperintense lesion.

5) T2W/FLAIR findings: on the T2W/FLAIR imaging, dif-

ferent signal of the lesion compared with the normal tissue of the brain itself is classified as no lesion, hypointense, isointense, or hyperintense lesion.

6) Diffusion restriction: abnormal restricted diffusion, which can be identified from diffusion weighted imaging (DWI), is classified as no restricted diffusion, restricted diffusion of the wall of the lesion, restricted diffusion of the cavity of the lesion, and patchy restricted diffusion.

7) Enhancement: the enhancement pattern after gadolinium administration is classified as no enhancement, homogeneous, heterogeneous, rim enhancement, and target sign patterns. The target sign is defined as a ring-shaped zone of peripheral enhancement with a small eccentric enhancing nodule.

8) Mass effect: phenomenon in which brain lesion causes surrounding areas of brain structures to be compressed due to space taking lesion.

9) Leptomeningeal enhancement: define as enhancement of the pia mater or enhancement that extends into the subarachnoid spaces of the sulci and cisterns.

10) Ventriculitis: characteristic MRI findings of ventriculitis include intraventricular debris and pus, abnormal periventricular and subependymal signal intensity, and enhancement of the ventricular lining on conventional MRI sequences.

11) Hydrocephalus: define as an abnormal expansion of cavities (ventricles) within the brain that is caused by the accumulation of CSF.

Final Diagnosis

The final diagnosis was accessed from medical record, followed by ICD 10, based on history, neurological examination, laboratory data (blood for antigen, CSF culture, CSF specific antigen, CSF-PCR, CSF Indian-ink, CSF cytology, and pathological report), and therapeutic treatment. Without universally agreed-upon definition for IRIS, we used combination of Shelburne et al[9] criteria and Roberson et al[10] criteria to define the IRIS group, which was described as the patient who diagnosis of AIDS, treatment with anti-HIV medicines had led to an increase in CD4 T lymphocytes ($\geq$ 25 cells/mm^3), symptoms consistent with an infectious/inflammatory condition appeared while on antiretroviral therapy, and symptoms could not be explained by a newly acquired infection, by the expected clinical course of a previously recognized infectious agent, or by side effects of therapy.

Data Collection

The demographic data which were collected by reviewing from the medical record were recorded in data collection form including: hospital number (HN), age, gender, clinical presentation, T-helper/inducer count (CD4), and history of HAART.

Statistical Analysis

Statistical analysis was descriptive statistical analysis including categorical variables; gender, clinical presentation, history of HAART, and CD4 level were described by number and percentage. CT and MRI imaging features were described by number and percentage. Continuous variables (age) were summarized by mean ($\bar{X}$) and standard deviation (SD).

Results

Two hundred sixty-four seropositive HIV patients underwent CT brain. Two hundred patients were excluded from the study, 111 patients for no intracranial pathology 23 patients for known case of HIV related brain lesions, 29 atients for non-HIV related brain lesions, and 37 patients for missing or inadequate data. Consequently, the study population included 64 patients with 43 males and 21 females. The median age was 34.5 years (range, 18 - 71 years). All of them had neurologic symptoms. Most common presenting neurologic symptom was headache (31.3%). The median CD4 count was 42.5 cell/mm^3 (range, 4 - 1.184 cell/mm^3). Only 19 patients (29.7%) had received HAART during the onset of symptom.

One hundred twenty-seven seropositive HIV patients underwent MRI brain. There were 83 patients who were excluded from the study, 25 patients for no intracranial pathology, 17 patients for known case of HIV related brain lesions, 29 patients for non-HIV related brain lesions, and 12 patients for missing or inadequate

data. The study population included 44 patients with 29 males and 15 females. The median age was 36.5 years (range, 20 - 64 years). All of them had neurologic symptoms. Most common presenting neurologic symptom was hemiparesis/weakness (25%). The median CD4 count was 70.5 cell/mm^3 (range, 4 - 1,184 cell/mm^3). Only 15 patients (34.1%) had received HAART during the onset of symptom. Details of the patient data are shown in Table 1.

Table 1 Baseline Patient Characteristics

Characteristic	CT	MRI
Gender		
Male, No. (%)	43 (67.2)	29 (65.9)
Female, No. (%)	21 (32.8)	15 (34.1)
Age, median (range)	34.5 (18 - 71)	36.5 (20 - 64)
Clinical presentation		
Alteration of conscious, No. (%)	13 (20.3)	9 (20.45)
Seizure, No.	7 (10.9)	6 (13.6)
Weakness, No. (%)	10 (15.6)	11 (25)
Headache, No. (%)	20 (31.3)	5 (11.4)
Fever, No. (%)	10 (15.6)	4 (9.1)
Other neurologic symptoms, No. (%)	4 (6.3)*	9 (20.45)**
T-helper/inducer count (CD4), cell/mm^3		
< 200, No. (%)	50 (78.1)	34 (77.3)
> 200, No. (%)	14 (21.9)	10 (22.7)
Median (range)	42.5 (4 - 1184)	70.5 (4 – 1184)
HAART, No. (%)	19 (29.7)	15 (34.1)

Abbreviation: CT, computed tomography; HAART, highly active antiretroviral therapy; MRI, magnetic resonance imaging.

* Included impaired memory, left facial palsy, dysarthria, and blurring vision.

** Included behavioral change, blurring vision, diplopia, ophthalmoplegia, papilledema, aphasia, and ataxia.

Imaging Findings

Sixty-four HIV patients with HIV-related brain lesion were performed by CT of the brain, 29.7% cryptococcal infection, 18.8% tuberculous infection, 9.4% HIVE, 7.8% neurosyphilis, 6.3% toxoplasmosis, 4.7% PML and tuberculosis-immune reconstitution inflammatory syndrome (TB-IRIS), and other cases of PCNSL, HSV, HIV vasculopathy, cytomegalovirus (CMV), varicella-zoster-virus (VZV), Microbacterium avium complex (MAC), histoplasmosis infection, combined diagnoses of toxoplasmosis and neurosyphilis, combined diagnoses of toxoplasmosis and tuberculosis, PML-IRIS, VZV-IRIS, and HIVE-IRIS. Details of the HIV-related brain lesions in each modalities are shown in Table 2.

Table 2 HIV-Related Brain Lesions in Each Modality

Disease	No. (%)		
	CT	MRI	Total
Cryptococcal infection	19 (29.7)	3 (6.8)	20 (24.7)
Tuberculous infection	12 (18.8)	10 (22.7)	15 (18.5)
HIV encephalopathy	6 (9.4)	2 (4.5)	7 (8.6)
PML	3 (4.7)	7 (15.9)	7 (8.6)
Neurosyphilis	5 (7.8)	2 (4.5)	6 (7.4)
Toxoplasmosis	4 (6.3)	3 (6.8)	5 (6.2)
PCNSL	1 (1.6)	2 (4.5)	2 (2.5)
HSV	1 (1.6)	1 (2.3)	1 (1.2)
HIV vasculopathy	1 (1.6)	1 (2.3)	1 (1.2)
CMV	1 (1.6)	1 (2.3)	1 (1.2)
VZV	1 (1.6)	1 (2.3)	1 (1.2)
Histoplasmosis infection	1 (1.6)	0	1 (1.2)
MAC	1 (1.6)	1 (2.3)	1 (1.2)
Toxoplasmosis and syphilis	1 (1.6)	1 (2.3)	1 (1.2)
Toxoplasmosis and tuberculosis	1 (1.6)	1 (2.3)	1 (1.2)
Tuberculosis and syphilis	0 (0)	1 (2.3)	1 (1.2)
Tuberculosis and HSV	0 (0)	1 (2.3)	1 (1.2)
TB-IRIS	3 (4.7)	3 (6.8)	5 (6.2)
PML-IRIS	1 (1.6)	1 (2.3)	1 (1.2)
HIVE-IRIS	1 (1.6)	0 (0)	1 (1.2)
VZV-IRIS	1 (1.6)	1 (2.3)	1 (1.2)
CMV-IRIS	0 (0)	1 (2.3)	1 (1.2)
Total	64 (100)	44 (100)	81 (100)

The patients who underwent both CT and MRI studies were calculated at 1 patient in total cases.

Forty-four HIV patients were performed by MRI of the brain, 22.7% tuberculous infection, 15.9% PML, 6.8% cryptococcal infection, toxoplasmosis, and TB-IRIS, 4.5% HIVE, neurosyphilis, and PCNSL, and other cases of HSV, HIV vasculopathy, CMV, VZV, MAC, combined diagnoses of toxoplasmosis and neurosyphilis, combined diagnoses of toxoplasmosis and tuberculosis, combined diagnoses of tuberculosis and neurosyphilis, combined diagnoses of tuberculosis and HSV, PML-IRIS, VZV-IRIS, and CMV-IRIS.

The most common diagnosis in this study was cryptococcal infection in 19 patients (29.7%). Common CT findings were no brain parenchymal lesion (78.9%), leptomeningeal enhancement (42.1%), and normal brain (42.1%). All cases of the brain lesion (21.1%) showed focal distribution, seen as a non-enhancing hypodense lesion at basal ganglia in 2 cases (10.5%), enhancing hyperdense lesion in 1 case, and non-enhancing hypodense lesion in 1 case. By MRI, diagnosed cryptococcal infection were performed in 3 patients (6.8%). One case showed diffuse multiple small non-enhancing hyperintense-T2 nodules with restricted diffusion, more on bilateral frontal lobes, suggestive of cryptococcal pseudocysts (Figure 1). One case showed subacute infarction of the lenticulostriate territory. The other showed a rim-enhancing hypointense-T1 and hyperintense-T2 lesion with perilesional edema, suggestive of cryptococcoma (Figure 2). Leptomeningeal enhancement was observed in two cases.

Diagnosed tuberculous infection patients were performed by CT of the brain in 12 cases (18.8%). Tuberculous meningitis was diagnosed in 8 patients (12.5%). Common CT findings were no brain parenchymal lesion (75%) and leptomeningeal enhancement (62.5%). One case showed basal meningitis (Figure 3). Only 25% of the patients showed normal brain study. All cases of the brain parenchymal lesion showed focal non-enhancing hypodense lesions, likely due to cortical infarction. Tuberculoma was diagnosed in 3 patients (4.7%). Two of them (67%) showed a focal rim-enhancing lesion, likely caseous tuberculoma (Figure 4). One case also showed mild mass effect and associated leptomeningeal enhancement. Another case showed multiple non-enhancing hypodense lesions. Tuberculous abscess was diagnosed in 1 patient and showed a large rim-enhancing hypodense lesion with mass effect and associated leptomeningeal enhancement (Figure 5). Tuberculous infection was the most common diagnosis and was diagnosed in 10 patients (18.5%) who performed by MRI. Six patients (13.6%) were tuberculous meningitis and all of them showed leptomeningeal enhancement with 2 cases showed basal meningitis (Figure 3). Three cases showed multifocal hypointense-T1 and hyperintense-T2 lesions with patchy diffusion restriction and gyral enhancement, suggestive of subacute infarctions of multiple vascular territories. Subpial enhancing nodules was found in 1 case. Tuberculoma was seen in 3 patients (6.8%). All cases showed nodular enhancing, hypo to isointense-T1 and hyperintense-T2 lesions with one case showed rim enhancement (Figure 4). Associated leptomeningeal enhancement was found in one case. Tuberculous abscess was seen in 1 case and showed a rim-enhancing lesion with cavitary restricted diffusion and mass effect.

Six HIVE patients (9.4%) were performed by CT. All of them showed diffuse brain atrophy (Figure 6). Diffuse symmetrical non-enhancing hypodense lesion at bilateral cerebral white matter were found in 50% of the patients and another half showed no brain lesion. Two HIVE patients (4.5%) were performed by MRI. All of the HIVE cases showed brain atrophy with diffuse hypointense-T1 and hyperintense-T2 lesions involving bilateral cerebral white matter. No enhancement or mass effect was observed (Figure 6).

Three PML patients (4.7%) were performed by CT. Two of them (66.7%) showed diffuse asymmetrical multiple hypodense lesions involving subcortical white matter (Figure 7) and 1 patient showed mass effect. Another case showed a focal hypodense lesion without mass effect. None of them showed enhancement. PML was found in 7 patients (15.9%) by MRI. All cases showed

multiple asymmetrical non-enhancing hypointense-T1 and hyperintense-T2 lesions involving bilateral subcortical white matter (Figure 7). Three cases showed wall and patchy diffusion restriction and one case showed mild mass effect and focal leptomeningeal enhancement.

Diagnosed neurosyphilis was performed by CT in 5 patients (7.8%). One of them showed multifocal non-enhancing hypodense lesions, which could be subcortical infarctions. The others showed normal CT brain. By MRI, 2 neurosyphilis cases were found (4.5%). One of them showed multifocal gyral enhancement due to cortical infarction in multiple territories. Another case showed enhancing nodule at vestibulocochlear nerve (Figure 8).

Four toxoplasmosis patients (6.3%) were performed by CT. All of them showed focal distribution of brain lesion with mass effect and marked perilesional edema. About 75% of the patients showed solitary or multiple rim-enhancing hypodense lesions. Another showed multiple patchy enhancing hypodense lesion. Most of the lesions involved corticomedullary junction and cerebellum (Figure 9). Associated leptomeningeal enhancement was found in one case. Three patients were performed by MRI. All of them showed multiple enhancing lesions with mass effect. Variability of enhancement pattern was observed, 2 cases showed ring and eccentric target enhancing patterns and another case showed heterogeneous and nodular enhancement (Figure 10). Associated leptomeningeal enhancement was found in 2 patients.

PCNSL was found in one case by CT. The CT findings was a focal faint enhancing, iso to hyperdense lesion at cerebral cortex with mass effect and leptomeningeal enhancement (Figure 11). PCNSL was diagnosed in 2 patients (4.5%) by MRI, showed a solitary hypointense-T1 and hyperintense-T2 lesion with wall restricted diffusion and rim enhancement at cerebral cortex and cerebellum, as well as hydrocephalus (Figure 12).

Other brain lesions were found. The case of HSV infection showed focal patchy enhancing hypodense lesions with leptomeningeal enhancement and hydrocephalus by CT and showed more details of multifocal acute to subacute infarctions of multiple vascular territories with diffuse leptomeningeal enhancement and mild hydrocephalus by MRI (Figure 13). By CT, the HIV vasculopathy case showed multifocal non-enhancing hypo and hyperdense lesions with leptomeningeal and gyral enhancement along the cerebral hemisphere and basal cistern, likely multifocal subacute infarctions. By MRI, the case showed multifocal acute and subacute infarctions of multiple vascular territories with leptomeningeal enhancement (Figure 14). The VZV infection showed multifocal non-enhancing hypodense lesions with mass effect, which more clarify as multifocal acute to subacute infarctions of left MCA territory by MRI (Figure 15). Associated leptomeningeal enhancement was also noted. The CMV infection showed brain atrophy with leptomeningeal enhancement, ventriculitis and hydrocephalus without focal brain lesion by both CT and MRI (Figure 16). The MAC infection showed a focal non-enhancing hypodense lesion with mass effect, leptomeningeal enhancement and hydrocephalus. By MRI, the case showed multifocal rim enhancing hypointense-T1 and isointense-T2 lesions with cavitary restricted diffusion, leptomeningeal enhancement and ventriculitis (Figure 17). Histoplasmosis infection showed a rim-enhancing hyperdense lesion at left frontal lobe with leptomeningeal enhancement and hydrocephalus by CT (Figure 18).

Combined diagnosis was also seen. Combined diagnoses of tuberculosis and neurosyphilis case showed a homogeneous enhancing hypodense lesion involving left middle cerebellar peduncle and left sided dorsal pons, suggestive of rhombencephalitis by CT. By MRI, the case showed patchy enhancing hypointense-T1 and hyperintense-T2 lesions with patchy restricted diffusion, cranial nerve enhancement and leptomeningeal enhancement. Combined diagnoses of toxoplasmosis and tuberculosis case showed multifocal non-enhancing hypodense lesions with mass effect, leptomeningeal enhancement, and hydrocephalus by CT and showed diffuse innumerous rim and nodular enhancing lesions with restricted diffusion

scattered at both cerebral hemispheres by MRI. Combined diagnoses of toxoplasmosis and neurosyphilis case showed multifocal acute to subacute infarctions with leptomeningeal enhancement. Combined diagnoses of tuberculosis and herpes simplex virus showed diffuse hyperintense-T2 lesions with basal leptomeningeal enhancement and hydrocephalus.

There are 9 cases of CNS-IRIS, which are TB-IRIS (3 patients), PML-IRIS, VZV-IRIS, HIVE-IRIS, and CMV-IRIS. One of TB-IRIS case showed extensive basal leptomeningeal enhancement and a focal rim-enhancing hypodense mass with extensive perilesional edema (Figure 19). The other cases showed leptomeningeal enhancement, except one case with normal CT brain. By MRI, all cases showed multifocal rim with/without nodular enhancing lesions with leptomeningeal enhancement. One case showed extensive basal meningitis and brain edema (Figure 20). The PML-IRIS case showed normal CT brain but diffuse multiple mild heterogeneous enhancing isointense-T1/hyperintense-T2 lesions without mass effect were found by MRI (Figure 21). The VZV-IRIS cases also showed normal CT brain but acute and subacute infarctions of multiple vascular territories were found by MRI (Figure 22). The HIVE-IRIS showed multifocal rim-enhancing hypodense lesions with mass effect and extensive basal leptomeningeal enhancement (Figure 23). The CMV-IRIS showed brain atrophy with multiple nodular lesions along the ependymal surface of bilateral lateral ventricle, leptomeningeal enhancement, and hydrocephalus without brain lesion.

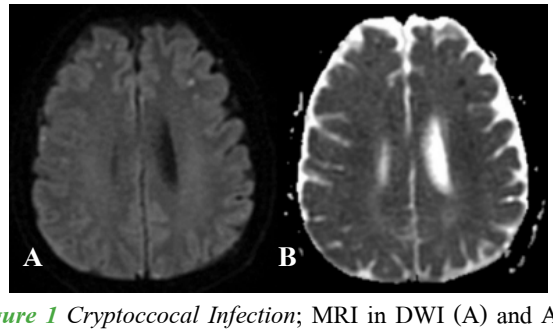

Figure 1 *Cryptoccocal Infection*; MRI in DWI (A) and ADC mapping (B) showed multiple restricted nodular lesion, suggestive of cryptococcal pseudocysts.

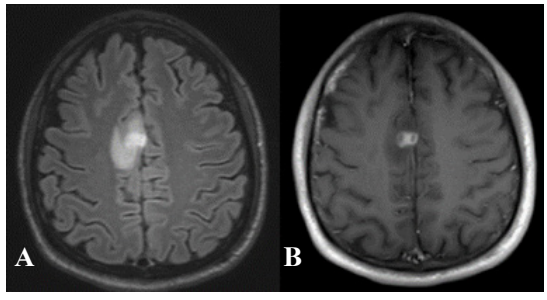

Figure 2 *Cryptoccocal Infection*; MRI in FLAIR image (A) and T1W image post gadolinium (B) showed a rim-enhancing hyperintense-T2 lesion with perilesional edema, suggestive of cryptococcoma.

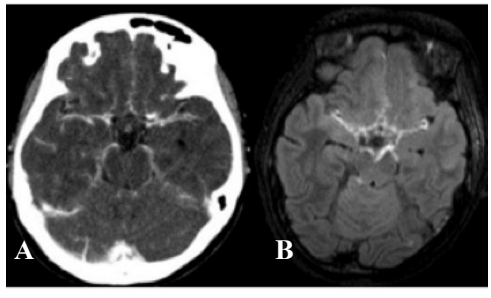

Figure 3 *Tuberculous Meningitis*; CT with contrast (A) and MRI in FLAIR image post gadolinium (B) demonstrated basal leptomeningeal enhancement.

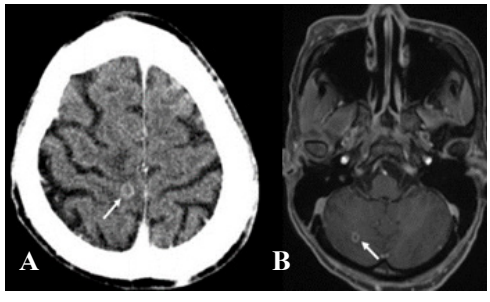

Figure 4 *Tuberculoma*; CT with contrast (A) and MRI in T1W image post gadolinium (B) demonstrated focal rim-enhancing lesion, likely caseous tuberculoma.

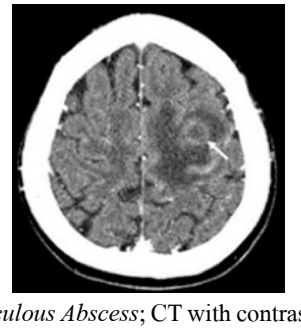

Figure 5 *Tuberculous Abscess*; CT with contrast showed a large rim-enhancing hypodense lesion with mass effect and associated leptomeningeal enhancement.

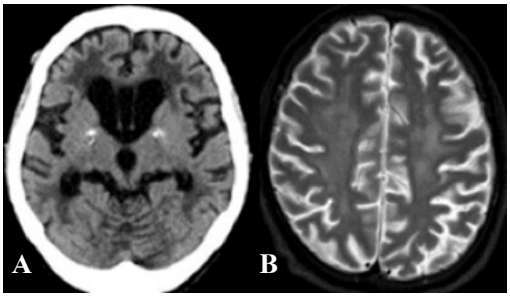

Figure 6 *HIV Encephalopathy*; CT brain (A) showed diffuse brain atrophy. MRI T2W-image (B) showed brain atrophy with diffuse hyperintense-T2 lesions involving bilateral cerebral white matter.

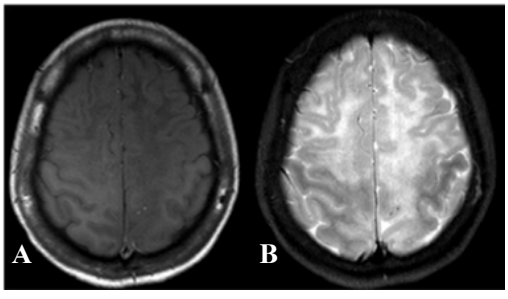

Figure 7 *PML*; MRI in T1W image (A) and T2W image (B) showed asymmetrical non-enhancing hypointense-T1 and hyperintense-T2 lesions involving bilateral subcortical white matter.

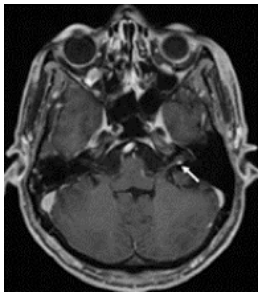

Figure 8 *Neurosyphilis*; MRI in T2W image showed a tiny enhancing nodule at vestibulocochlear nerve

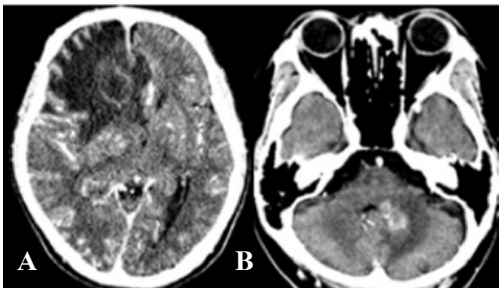

Figure 9 *Toxoplasmosis*; CT brain (A) showed a focal rim-enhancing lesion with mass effect and markedly perilesional edema. Another CT brain (B) showed a rim-enhancing hypodense nodules at left middle cerebellar peduncle.

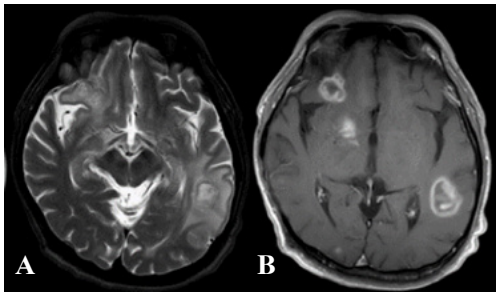

Figure 10 *Toxoplasmosis*; MRI of the brain in T2W image (A), and T1W post gadolinium (B) showed multiple eccentric target enhancing lesions with mass effect.

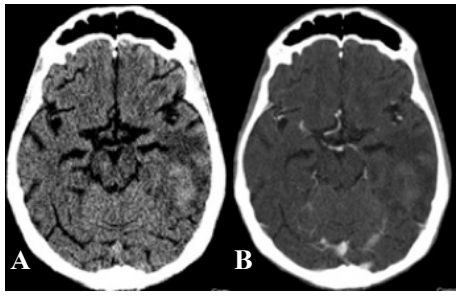

Figure 11 *PCNSL*; CT brain; plain (A) and post contrast (B) showed focal faint enhancing hyperdense lesion at left temporal lobe with mass effect and leptomeningeal enhancement.

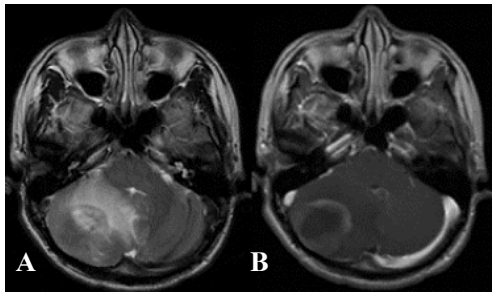

Figure 12 *PCNSL*; MRI of the brain in T2W image (A), and T1W post gadolinium (B) showed a rim-enhancing hyperintense-T2 lesion at right cerebellum.

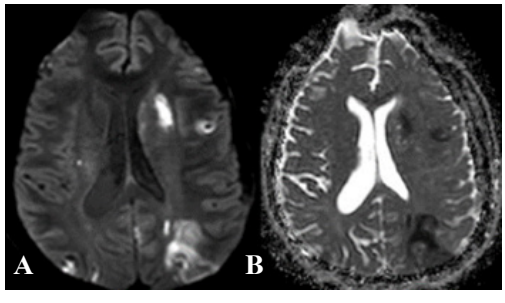

Figure 13 *HSV Infection*; MRI in DWI (A) and ADC mapping (B) showed multifocal acute to subacute infarctions of multiple vascular territories.

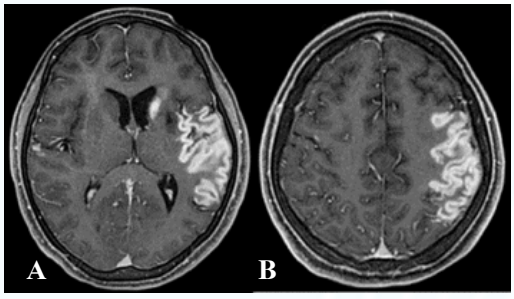

Figure 14 *HIV Vasculopathy*; MRI in T1W post gadolinium showed multifocal infarctions with gyral enhancement

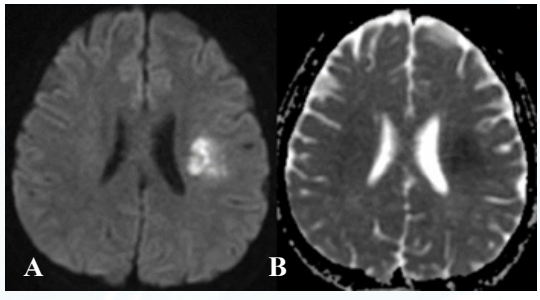

Figure 15 *VZV Vasculopathy*; MRI in DWI (A) and ADC mapping (B) showed acute to subacute infarctions of left MCA territory.

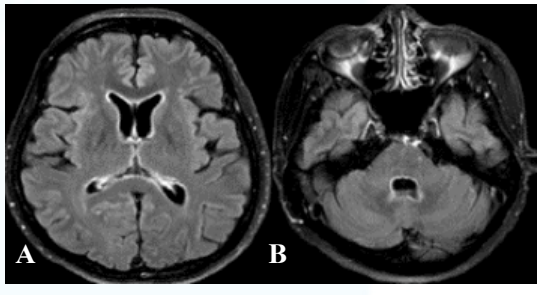

Figure 16 *CMV Infection*; MRI in FLAIR image post gadolinium (A, B) showed diffuse atrophic change of brain parenchyma with leptomeningeal enhancement, ventriculitis and hydrocephalus.

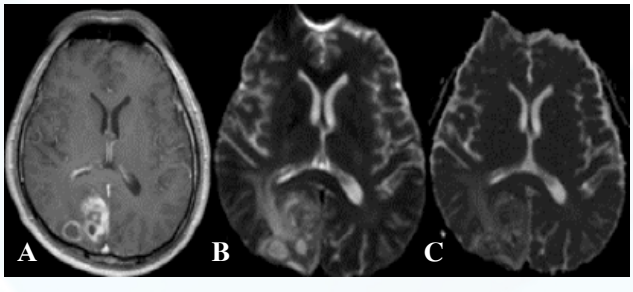

Figure 17 *MAC Infection*; MRI of the brain in T1W post gadolinium (A), DWI (B) and ADC mapping (C) showed multiple rim-enhancing lesions with cavitary restricted diffusion, likely brain abscess.

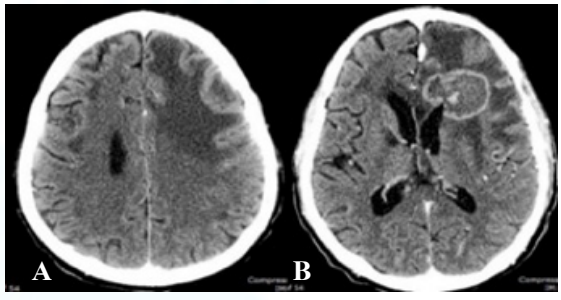

Figure 18 *Histoplasmosis Infection*; CT brain post contrast showed a rim-enhancing hyperdense lesion at left frontal lobe with leptomeningeal enhancement.

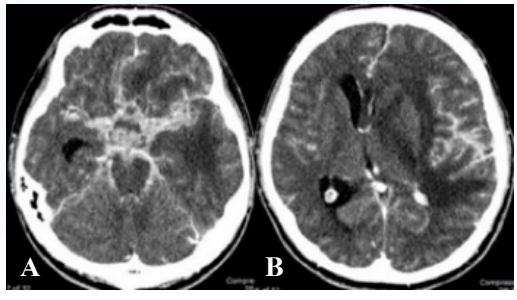

Figure 19 *TB-IRIS*; CT brain post contrast (A, B) showed extensive basal leptomeningeal enhancement and a focal rim-enhancing hypodense mass with extensive perilesional edema.

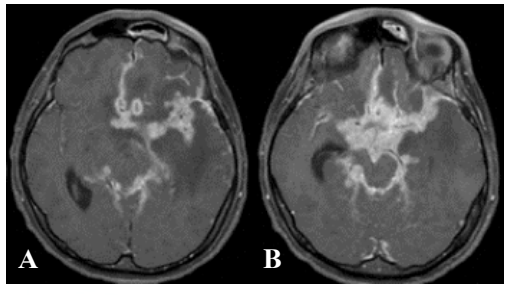

Figure 20 *TB-IRIS*; MRI in T1W images (A, B) post gadolinium showed rim-enhancing lesion with extensive basal meningitis and brain edema.

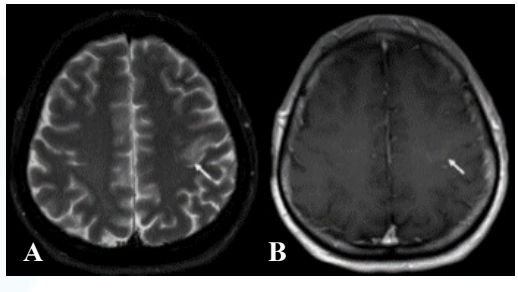

Figure 21 *PML-IRIS*; MRI in T2W image (A) and T1W post gadolinium (B) showed mild heterogeneous enhancing hyperintense-T2 lesion without mass effect.

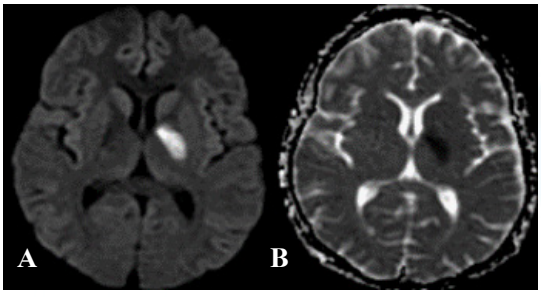

Figure 22 *VZV-IRIS*; MRI in DWI (A) and ADC mapping (B) showed acute infarction of the lenticulostriate branch of the left MCA, seen as non-enhancing lesion with restricted diffusion involving posterior limb of the left internal capsule and left globus pallidus.

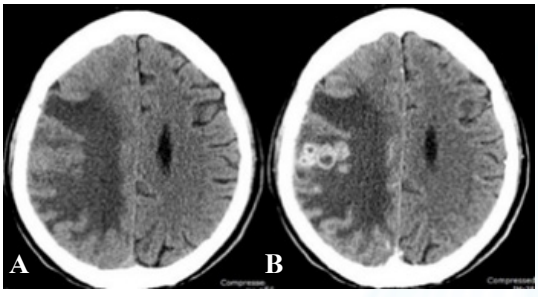

Figure 23 *HIVE-IRIS*; CT brain; plain (A) and post contrast (B) showed multifocal rim-enhancing hypodense lesions with mass effect.

Discussion

Eighty-one HIV-related brain lesions were diagnosed, including 24.7% cryptococcal infection, 18.5% tuberculous infection, 8.6% HIV encephalopathy and PML, 7.4% neurosyphilis, 6.2% toxoplasmosis and TB-IRIS, 2.5% PCNSL, and other cases of HSV, HIV vasculopathy, CMV, VZV, MAC, histoplasmosis, combined diagnoses of toxoplasmosis and neurosyphilis, combined diagnoses of toxoplasmosis and tuberculosis, combined diagnoses of tuberculosis and neurosyphilis, combined diagnoses of tuberculosis PML-IRIS, VZV-IRIS, CMV-IRIS, and HIVE-IRIS. There were prior studies about HIV-related brain lesions showing variation in diseases and incidence, which may be due to different geographic areas, period of evaluation, and different inclusion criteria.[1, 3-7, 8-10]

Majority of the imaging findings of HIV-related brain lesions were not different from the prior studies. All cases of HIVE showed brain atrophy.[11] CNS cryptococcal infection showed no focal brain lesion (75%) and 45% showed leptomeningeal enhancement. Hypodense lesion by CT of the brain at basal ganglia, which could be gelatinous pseudocyst, or old lacunar infarction, was found in only few cases. All findings by MRI were consistent with the prior studies.[12] Most of findings seen in the cases of tuberculous infection were consistent with the previous studies, including leptomeningeal enhancement (90%), without brain lesion (50%). Basal meningitis was found only 3 cases (30%). By MRI, multifocal subacute infarctions were found in 50%, suggestive of basal vasculitis. Tuberculoma showed a focal rim-enhancing lesion with or without mass effect in 2 cases, suggested caseous tuberculoma. Nodular enhancing lesions were found in all cases, suggested non-caseating tuberculoma. A rim-enhancing lesion was also detected in 1 case. Associated leptomeningeal enhancement was found in 50%. A case of tuberculous abscess showed a large rim-enhancing hypodense/isointense-T1 and hyperintense-T2 lesion with cavitary restricted diffusion and mass effect.[13-14] However, basal meningitis was incommon, hydrocephalus and target lesion were not found in this study. All of toxoplasmosis cases showed focal lesion(s) (80% multiple) with mass effect and marked perilesional edema. Rim-enhancing hypodense lesions involved corticomedullary junction and cerebellum are common presentation in CT findings. By MRI, ring and eccentric target enhancing pattern (eccentric target sign) were common but heterogeneous and nodular enhancement could be found.

From the prior study, eccentric target sign, which is composed of concentrically thickened vessels traversing the sulcus produced the eccentric target enhancement, surrounding zone of necrosis produced the intermediate zone of hypointensity and enhancing rim from histiocyte response with inflamed and proliferating vessels, was considered with 95% specificity and 25% sensitivity for diagnosis of toxoplasmosis.[16-17] In our study, it was found in 66.7% and was not found in other diseases. Due to relatively common question to distinguish between cerebral

toxoplasmosis and PCNSL in HIV patients,difference between these two diseases were found in many findings, such as multiplicity, location, increased attenuation in non-contrasted CT in PCNSL, restricted diffusion in PCNSL, eccentric target sign in toxoplasmosis.[18-19] In the present study, most of PML cases showed asymmetrical multiple hypodense lesions in CT and hyperdense-T2 lesions involving bilateral subcortical white matters without mass effect or enhancement. However, mild mass effect was also found in two cases and focal leptomeningeal enhancement was found in one case, who not on antiretroviral therapy prior to presentation. These atypical findings were also reported infrequently in prior studies.

The other rare HIV-related brain lesions were found in the present study, including HSV infection, HIV vasculopathy, VZV infection, CMV infection, MAC infection, and histoplasmosis. These findings were consistent with prior studies.[20-22]

Concomitant HIV-related brain lesions, the imaging findings are compatible with the prior study, including toxoplasmosis and neurosyphilis infection,[15] concomitant toxoplasmosis and tuberculosis, toxoplasmosis and neurosyphilis and tuberculosis and herpes simplex virus.

Nine cases of CNS-IRIS were found and were compatible with the prior studies. The HIVE-IRIS was diagnosed in one case and showed multifocal rim-enhancing lesions with mass effect and extensive basal leptomeningeal enhancement. The findings were difference from radiographic appearances of HIVE and other HIVE-IRIS cases from prior literature, which are seen as diffuse bilateral high T2 lesions at both white and gray matter, multiple punctate or linear enhancement, and infrequently fulminant focal area of demyelination or tumefactive inflammation.[23] Five cases of TB-IRIS were diagnosed, which had variable imaging findings. One case showed extensive leptomeningeal enhancement and a rim-enhancing mass with extensive perilesional edema. While the other 2 cases showed focal enhancing lesions with leptomeningeal enhancement, similar to imaging findings of tuberculous infection. One of the cases showed only leptomeningeal enhancement and another case show normal CT. One case of PML-IRIS showed diffuse enhancing hyperintense-T2 lesions without mass effect, which is consistent with a prior study and not different from atypical PML case. The VZV-IRIS case showed normal CT brain. The CMV-IRIS case showed leptomeningeal enhancement and hydrocephalus without focal parenchymal lesion, not different from the CMV case.[24]

Limitation of study included a retrospective nature resulted in some missing clinical information, small sample size, multiple diversities of HIV-related brain lesions, and incomplete surgical or pathological confirmation.

Conclusions

The most common disease of adult HIV-related brain lesions in Ramathibodi Hospital was cryptococcal infection, followed by tuberculous infection, HIV encephalopathy, and PML. Besides less basal meningitis and hydrocephalus in tuberculous meningitis and no demonstrated target lesion in tuberculoma compared with prior literatures, other imaging findings of each HIV-related brain lesions were not different. Some findings were found to be helpful for diagnosis of some diseases, such as brain atrophy without focal lesion in HIV encephalopathy, asymmetrical non-enhancing hypodense or hyperintense-T2 lesions at bilateral subcortical white matter in PML, and eccentric target sign in toxoplasmosis.

Diagnosis of CNS-IRIS was still difficult due to variable of imaging findings. The appearances on neuroimaging studies, such as extensive lesions, contrast enhancement, or mass effect in infections should raise suspicion for diagnosis of IRIS. However, imaging findings similar to each disease or even normal brain study cannot rule out diagnosis of IRIS.

References

1. Smith AB, Smirniotopoulos JG, Rushing EJ. From the archives of the AFIP: central nervous system infections associated with human immunodeficiency virus infection: radiologic-pathologic correlation. *Radiographics*. 2008;28(7):2033-2058. doi:10.1148/rg.287085135.
2. UNAIDS/WHO. *Fact sheet: 2014 statistics*. Geneva, Switzerland: World Health Organization, 2014.
3. Maschke M, Kastrup O, Esser S, Ross B, Hengge U, Hufnagel A. Incidence and prevalence of neurological disorders associated with HIV since the introduction of highly active antiretroviral therapy (HAART). *J Neurol Neurosurg Psychiatry*. 2000;69(3):376-380.
4. Masliah E, DeTeresa RM, Mallory ME, Hansen LA. Changes in pathological findings at autopsy in AIDS cases for the last 15 years. *AIDS*. 2000;14(1):69-74.
5. Burns DK, Risser RC, White CL. The neuropathology of human immunodeficiency virus infection. The Dallas, Texas, experience. *Arch Pathol Lab Med*. 1991;115(11):1112-1124.
6. Hongsakul K, Laothamatas J. Computer tomographic findings of the brain in HIV-patients at Ramathibodi Hospital. *J Med Assoc Thai*. 2008;91(6):895-907.
7. Post MJ, Thurnher MM, Clifford DB, et al. CNS-immune reconstitution inflammatory syndrome in the setting of HIV infection, part 1: overview and discussion of progressive multifocal leukoencephalopathy-immune reconstitution inflammatory syndrome and cryptococcal-immune reconstitution inflammatory syndrome. *AJNR Am J Neuroradiol*. 2013;34(7):1297-1307. doi:10.3174/ajnr.A3183.
8. Post MJ, Thurnher MM, Clifford DB, et al. CNS-immune reconstitution inflammatory syndrome in the setting of HIV infection, part 2: discussion of neuro-immune reconstitution inflammatory syndrome with and without other pathogens. *AJNR Am J Neuroradiol*. 2013;34(7):1308-1318. doi:10.3174/ajnr.A3184.
9. Shelburne SA, Hamill RJ, Rodriguez-Barradas MC, et al. Immune reconstitution inflammatory syndrome: emergence of a unique syndrome during highly active antiretroviral therapy. *Medicine (Baltimore)*. 2002;81(3):213-227.
10. Robertson J, Meier M, Wall J, Ying J, Fichtenbaum CJ. Immune reconstitution syndrome in HIV: validating a case definition and identifying clinical predictors in persons initiating antiretroviral therapy. *Clin Infect Dis.* 2006;42(11):1639-1646.
11. Post MJD, Tate LG, Quencer RM et al. CT, MR, and pathology in HIV encephalitis and meningitis. *AJR Am J Roentgenol.* 1988;151:373-380.
12. Offiah CE, Naseer A. Spectrum of imaging appearances of intracranial cryptococcal infection in HIV/AIDS patients in the anti-retroviral therapy era. *Clin Radiol*. 2016;71(1):9-17. doi:10.1016/j.crad.2015.10.005.
13. Nelson CA, Zunt JR. Tuberculosis of the Central nervous system in immunocompromised patients: HIV infection and solid organ transplant recipients. *Clin Infect Dis*. 2011;53(9):915-926. doi:10.1093/cid/cir508.
14. Trivedi R, Saksena S, Gupta RK. Magnetic resonance imaging in central nervous system tuberculosis. Indian *J Radiol Imaging*. 2009;19(4):256-265. doi:10.4103/0971-3026.57205.
15. Smith MM, Andersona JC. Neurosyphilis as a cause of facial and vestibulocochlear nerve dysfunction: MR imaging features. *AJNR Am J Neuroradiol.* 2000;21(9):1673-1675.
16. Kumar GG, Mahadevan A, Guruprasad AS, et al. Eccentric target sign in cerebral toxoplasmosis: neuropathological correlate to the imaging feature. *J Magn Reson Imaging*. 2010;31(6):1469-1472. doi:10.1002/jmri.22192.
17. Mahadevan A, Ramalingaiah AH, Parthasarathy S, Nath A, Ranga U, Krishna SS. Neuropathological correlate of the "concentric target sign" in MRI of HIV-associated cerebral toxoplasmosis. *J Magn Reson Imaging*. 2013;38(2):488-495. doi:10.1002/jmri.24036.

References

18. Haldorsen IS, Espeland A, Larssonc EM. Central nervous system lymphoma: characteristic findings on traditional and advanced imaging. *AJNR Am J Neuroradiol*. 2011;32(6):984-992. doi:10.3174/ajnr.A2171.
19. Dina TS. Primary central nervous system lymphoma versus to xoplasmosis in AIDS. *Radiology*. 1991;179(3):823-828.
20. Tan IL, McArthur JC, Venkatesan A, Nath A. Atypical manifestations and poor outcome of herpes simplex encephalitis in the immunocompromised. *Neurology*. 2012;79(21):2125-2132. doi:10.1212/WNL.0b013e3182752ceb.
21. Begley C, Amaraneni A, Lutwick L. Mycobacterium avium-intracellulare brain abscesses in an HIV-infected patient. *IDCases*. 2015;2(1):19-21.
22. Hariri OR, Minasian T, Quadri SA, et al. Histoplasmosis with deep CNS involvement: case presentation with discussion and literature review. *J Neurol Surg Rep*. 2015;76(1):e167-e172. doi:10.1055/s-0035-1554932.
23. Lindzen E, Jewells V, Bouldin T, Speer D, Royal W, Markovic-Plese S. Progressive tumefactive inflammatory central nervous system demyelinating disease in an acquired immunodeficiency syndrome patient treated with highly active antiretroviral therapy. *J Neurovirol*. 2008;14(6):569-573. doi:10.1080/13550280802304753.
24. Bahr N, Boulware DR, Marais S, Scriven J, Wilkinson RJ, Meintjes G. Central nervous system immune reconstitution inflammatory syndrome. *Curr Infect Dis Rep*. 2013;15(6):583-596. doi:10.1007/s11908-013-0378-5.

Original Article/นิพนธ์ต้นฉบับ

การศึกษาภาพเอกซเรย์คอมพิวเตอร์และสนามแม่เหล็กไฟฟ้าสมองของผู้ป่วยเอดส์ที่มารับการตรวจ ณ โรงพยาบาลรามาธิบดี

วิบูลย์ สุริยจักรยุทธนา[1], วัณณิตา มยุระสาคร[1], อังสนา ภู่เผือกรัตน์[2], ปวิน นำธวัช[3]

[1] ภาควิชารังสีวิทยา คณะแพทยศาสตร์โรงพยาบาลรามาธิบดี มหาวิทยาลัยมหิดล

[2] ภาควิชาอายุรศาสตร์ คณะแพทยศาสตร์โรงพยาบาลรามาธิบดี มหาวิทยาลัยมหิดล

[3] กลุ่มสาขาวิชาระบาดวิทยาคลินิกและชีวสถิติ คณะแพทยศาสตร์โรงพยาบาลรามาธิบดี มหาวิทยาลัยมหิดล

บทคัดย่อ

บทนำ: ระบบประสาทส่วนกลางเป็นระบบสำคัญในการเกิดโรคแทรกซ้อนในผู้ป่วยเอดส์ รังสีวิทยาวินิจฉัยมีบทบาทสำคัญในการวินิจฉัยและการรักษาโรค ปัจจุบันมีการรักษาผู้ป่วยเอดส์ด้วยยาต้านไวรัสที่มีประสิทธิภาพสูง ทำให้เกิดภาวะฟื้นตัวของระบบภูมิคุ้มกัน และภาพวินิจฉัยที่แตกต่างไป

วัตถุประสงค์: เพื่อศึกษาภาพเอกซเรย์คอมพิวเตอร์และสนามแม่เหล็กไฟฟ้าสมองของโรคแทรกซ้อนที่เกิดและไม่เกิดร่วมกับภาวะฟื้นตัวของระบบภูมิคุ้มกันในผู้ป่วยเอดส์ของโรงพยาบาลรามาธิบดี

วิธีการศึกษา: ทำการศึกษาย้อนหลังผู้ป่วยเอดส์อายุ 18 ปีขึ้นไป ที่ตรวจภาพเอกซเรย์คอมพิวเตอร์ และ/หรือ สนามแม่เหล็กไฟฟ้าสมอง ก่อนการรักษา และวินิจฉัยโรคจากข้อมูลทางคลินิกต่างๆ

ผลการศึกษา: ผู้ป่วยเอดส์ จำนวน 81 คน ติดเชื้อราคริบโตค็อกคัสร้อยละ 24.7 วัณโรคร้อยละ 18.5% ไวรัสเอชไอวีของเนื้อสมองและไวรัสปาโปวาร้อยละ 8.6 ซิฟิลิสร้อยละ 7.4 โปรโตซัวชนิดท็อกโสพลาสมาร้อยละ 6.2 และวัณโรคสมองร่วมกับภาวะอักเสบจากภาวะฟื้นตัวของระบบภูมิคุ้มกันร้อยละ 6.2

สรุป: การติดเชื้อราคริบโตค็อกคัสของสมองพบมากที่สุดในผู้ป่วยเอดส์ของโรงพยาบาลรามาธิบดี ภาพทางรังสีวิทยามีลักษณะใกล้เคียงกับการศึกษาที่ผ่านมา ความผิดปกติที่มีมากขึ้น การสะสมของสารทึบรังสีมากขึ้น หรือมีการกดเบียดอวัยวะอื่นในโรคที่ไม่เคยพบลักษณะดังกล่าว ภาพทางรังสีของสมองจะช่วยในการวินิจฉัยการติดเชื้อของสมองร่วมกับภาวะฟื้นตัวของระบบภูมิคุ้มกัน

คำสำคัญ: เอกซเรย์คอมพิวเตอร์ การตรวจสนามแม่เหล็กไฟฟ้า ไวรัสเอชไอวี ภาวะฟื้นตัวของระบบภูมิคุ้มกัน การรักษาด้วยยาต้านไวรัสที่มีประสิทธิภาพสูง

Corresponding Author: วิบูลย์ สุริยจักรยุทธนา
ภาควิชารังสีวิทยา คณะแพทยศาสตร์โรงพยาบาลรามาธิบดี มหาวิทยาลัยมหิดล
270 ถนนพระรามที่ 6 แขวงทุ่งพญาไท เขตราชเทวี กรุงเทพฯ 10400
โทรศัพท์ +66 2201 1259 อีเมล wiboonsuriya@yahoo.com